

Plasmons in graphene: the nearest and next-nearest neighbor hopping

V. Kadirko¹, K. Ziegler² and E. Kogan¹

¹ *The Department of Physics,
Bar-Ilan University, Ramat Gan 52900, Israel*

² *Institute für Physik, Universität Augsburg
(Dated: November 3, 2011)*

The spectrum of plasmon excitations in graphene is studied in the framework of the tight-binding model, including nearest-neighbor and next-nearest-neighbor hopping. The dielectric function is numerically calculated as a function of wave vector and frequency, and two alternative approximations for calculating the plasmon dispersion law – the method based on the loss function and that based on the nullification of the real part of dielectric function – were used, compared and shown to agree with each other. It was also shown that next-nearest neighbor hopping may influence substantially the plasmon dispersion curve and/or the region of wave vectors where plasmons can be observed.

PACS numbers: 73.20.Mf

INTRODUCTION

Graphene, a single layer of carbon atoms arranged as a honeycomb lattice, is a semimetal with remarkable physical properties [1, 2]. This is due to the band structure of the material which consists of two bands which touch each other at two nodes. The electronic spectrum around these two nodes is linear and can be approximated by Dirac cones. Many unusual physical properties are controlled by the fact that the Fermi energy is at the nodes, where the density of states vanishes. However, graphene can be gated, so the Fermi energy can be freely tuned.

In the following we will discuss collective excitation of the 2D electron gas in graphene, caused by an external electromagnetic field. A standard problem in semiconductor physics, it was initially studied in the case of graphene only in the Dirac approximation around the nodes [3–5]. Later the results of calculations based on the full band structure, taken into account within the tight-binding model have appeared [6, 7]. We extend the nearest-neighbor approximation used in these papers by taking into account in addition the next-nearest-neighbor hopping.

We consider an electron gas which is subject to an electromagnetic potential $V_i(\mathbf{q}, \omega)$. The response of the electron gas is a screening potential $V_s(\mathbf{q}, \omega)$ which is caused by the rearrangement of the electrons due to external potential. Therefore, the total potential, acting on the electrons, is

$$V(\mathbf{q}, \omega) = V_i(\mathbf{q}, \omega) + V_s(\mathbf{q}, \omega). \quad (1)$$

V_s can be evaluated self-consistently and is expressed via the dielectric function $\epsilon(\mathbf{q}, \omega)$. Then the total potential reads

$$V(\mathbf{q}, \omega) = \frac{1}{\epsilon(\mathbf{q}, \omega)} V_i(\mathbf{q}, \omega). \quad (2)$$

ELEMENTARY ELECTRONIC PROPERTIES OF GRAPHENE

Graphene is made out of carbon atoms arranged in hexagonal structure. The structure can be seen as a triangular lattice with a basis of two atoms per unit cell (atom A and atom B). The tight-binding Hamiltonian

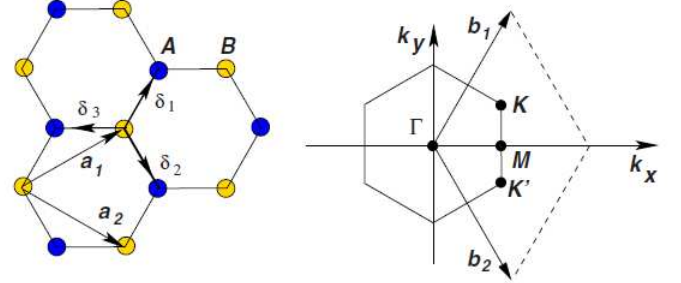


FIG. 1: A honeycomb lattice and its Brillouin zone. Left: lattice structure of graphene, made out of two interpenetrating triangular lattices (\mathbf{a}_1 and \mathbf{a}_2 are the lattice unit vectors, and δ_i , $i=1,2,3$ are the nearest-neighbor vectors). Right: corresponding Brillouin zone. The Dirac cones are located at the \mathbf{K} and \mathbf{K}' points.

for electrons in graphene with both nearest- and next-nearest-neighbor hopping has the form[1] (we use units such that $\hbar = 1$)

$$H = -t \sum_{\langle i,j \rangle, \sigma} (a_{\sigma,i}^\dagger b_{\sigma,j} + H.c.) - t' \sum_{\langle\langle i,j \rangle\rangle, \sigma} (a_{\sigma,i}^\dagger a_{\sigma,j} + b_{\sigma,i}^\dagger b_{\sigma,j} + H.c.) \quad (3)$$

where $a_{\sigma,i}$ ($a_{\sigma,i}^\dagger$) annihilates (creates) an electron with spin σ ($\sigma = \uparrow, \downarrow$) on site \mathbf{R}_i on sublattice A (an equivalent definition is used for sublattice B), $t \approx 2.8$ eV is the nearest-neighbor hopping energy (hopping between different sublattices), and t' is the next nearest-neighbor hopping integral (hopping in the same sublattice). The

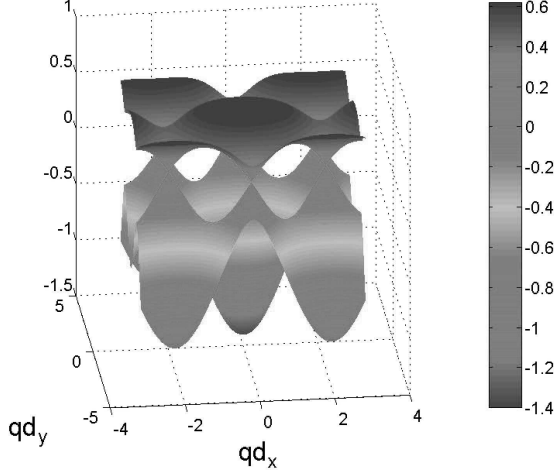


FIG. 2: Energy dispersion of graphene with $t' = 0.2t$. The figure shows a broken particle-hole symmetry. The Dirac nodes are shifted up by $3t'$. The energy is measured in the units of the electronic bandwidth $\Delta = 3t$.

value of t' is not well known but ab initio calculations find $0.02t \lesssim t' \lesssim 0.2t$ depending on the tightbinding parametrization [1].

The energy bands derived from this Hamiltonian have the form

$$E_{\pm}(\mathbf{k}) = \pm t \sqrt{3 + f(\mathbf{k})} - t' f(\mathbf{k}),$$

$$f(\mathbf{k}) = 2 \cos(\sqrt{3}k_y a) + 4 \cos\left(\frac{\sqrt{3}}{2}k_y a\right) \cos\left(\frac{3}{2}k_y a\right) \quad (4)$$

where the plus sign applies to the upper (π) and the minus sign the lower (π^*) band.

The expansion of the spectrum around the Dirac point \mathbf{K} including t' up to second order in q/K is given by

$$E_{\pm}(\mathbf{k}) \simeq 3t' \pm v_F |\mathbf{q}| - \left(\frac{9t'a^2}{4} \pm \frac{3ta^2}{8} \sin(3\theta_{\mathbf{q}}) \right) |\mathbf{q}|^2 \quad (5)$$

where $\theta_{\mathbf{q}} = \tan^{-1}(\frac{q_x}{q_y})$, and $\mathbf{q} = \mathbf{K} - \mathbf{k}$. Hence, the presence of t' shifts in energy the position of the Dirac point and breaks electron-hole symmetry.

DIRAC POINTS AND SADDLE POINTS

The Hamiltonian for a general two-sub-lattice lattice is

$$H = \begin{vmatrix} -\sum_{\mathbf{a}} t'(\mathbf{a}) e^{i\mathbf{k} \cdot \mathbf{a}} & -\sum_{\mathbf{a}} t(\mathbf{a} + \delta) e^{i\mathbf{k} \cdot (\mathbf{a} + \delta)} \\ -\sum_{\mathbf{a}} t^*(\mathbf{a} + \delta) e^{-i\mathbf{k} \cdot (\mathbf{a} + \delta)} & -\sum_{\mathbf{a}} t'(\mathbf{a}) e^{i\mathbf{k} \cdot \mathbf{a}} \end{vmatrix}, \quad (6)$$

where \mathbf{a} is an arbitrary lattice vector, and δ is a vector connecting two sites of different sub-lattices. The dispersion law thus is given by equation

$$F(E(\mathbf{k}), \mathbf{k}) \equiv \left[E(\mathbf{k}) + \sum_{\mathbf{a}} t'(\mathbf{a}) e^{i\mathbf{k} \cdot \mathbf{a}} \right]^2 - \left| \sum_{\mathbf{a}} t(\mathbf{a} + \delta) e^{i\mathbf{k} \cdot \mathbf{a}} \right|^2 = 0. \quad (7)$$

The conditions for the Dirac points are

$$\frac{\partial F}{\partial E(\mathbf{k})} = 0 \quad (8)$$

$$\frac{\partial F}{\partial \mathbf{k}} = 0. \quad (9)$$

Actually, in mathematics Dirac points we are dealing with are called conical points of the surface, and the condition (8) can be found in Ref. [8]. Eqs. (8) gives

$$E(\mathbf{k}) = - \sum_{\mathbf{a}} t'(\mathbf{a}) e^{i\mathbf{k} \cdot \mathbf{a}}; \quad (10)$$

Substituting this into Eq. (7) we get necessary condition of the Dirac point

$$\sum_{\mathbf{a}} t(\mathbf{a} + \delta) e^{i\mathbf{k} \cdot \mathbf{a}} = 0. \quad (11)$$

We also see that if \mathbf{k} satisfies Eq. (11), Eq. (9) is satisfied automatically. An interesting fact is that intra-sublattice hopping does not influence the position of Dirac points, but of course influences the value of energy in these points, which in general case is given by Eq. (10); in a particular model we are considering, this energy is $3t'$. The only symmetry which was essential for the Dirac point condition (11) was the sub-lattices symmetry (equality of diagonal matrix elements in the Hamiltonian (6)).

The critical points of the dispersion law surface described by Eq. (4) are found from the system

$$\frac{\partial f(\mathbf{k})}{\partial k_x} = 0, \quad \frac{\partial f(\mathbf{k})}{\partial k_y} = 0, \quad (12)$$

which has the solution corresponding to the Dirac points and 4 other

$$(0, 0), \quad \left(0, \frac{2\pi}{3a}\right), \quad \left(\frac{\pi}{3a}, \frac{\pi}{\sqrt{3}a}\right), \quad \left(\frac{\pi}{3a}, -\frac{\pi}{\sqrt{3}a}\right). \quad (13)$$

The values of f in these points are

$$6, -2, -2, -2. \quad (14)$$

The first solution corresponds to maximum of $f(k)$ (minimum of valence band and maximum of conduction band), the other three solutions are saddle points. The energy in these points is

$$E = \pm t + 2t'. \quad (15)$$

DIELECTRIC FUNCTION

The longitudinal dielectric function was calculated in Random Phase Approximation

$$\epsilon(\mathbf{q}, \omega) = 1 - \frac{2\pi e^2}{q\kappa} \chi(\mathbf{q}, \omega) \quad (16)$$

where κ is a dielectric constant and χ is a polarizability. For polarizability we used the Lindhard formula, which in our case after some straightforward calculations can be reduced to the expression

$$\chi(\mathbf{q}, \omega) = \chi_1(\mathbf{q}, \omega) + \chi_2(\mathbf{q}, \omega) \quad (17)$$

with the intraband contribution

$$\begin{aligned} \chi_1(\mathbf{q}, \omega) = & \lim_{\delta \rightarrow 0} \sum_{s,t=\pm 1} \int_{BZ} \frac{1}{4} |\kappa_{\mathbf{k}}^* \kappa_{\mathbf{k}+\mathbf{q}} + 1|^2 \\ & \times \frac{f(sE_{\mathbf{k}}^{(1)} + E_{\mathbf{k}}^{(2)})}{s(E_{\mathbf{k}}^{(1)} - E_{\mathbf{k}+\mathbf{q}}^{(1)}) + E_{\mathbf{k}}^{(2)} - E_{\mathbf{k}+\mathbf{q}}^{(2)} + t(\omega - i\delta)} d^2k, \end{aligned} \quad (18)$$

and the interband contribution

$$\begin{aligned} \chi_2(\mathbf{q}, \omega) = & \lim_{\delta \rightarrow 0} \sum_{s,t=\pm 1} \int_{BZ} \frac{1}{4} |\kappa_{\mathbf{k}}^* \kappa_{\mathbf{k}+\mathbf{q}} - 1|^2 \\ & \times \frac{f(sE_{\mathbf{k}}^{(1)} + E_{\mathbf{k}}^{(2)})}{s(E_{\mathbf{k}}^{(1)} + E_{\mathbf{k}+\mathbf{q}}^{(1)}) + E_{\mathbf{k}}^{(2)} - E_{\mathbf{k}+\mathbf{q}}^{(2)} + t(\omega - i\delta)} d^2k, \end{aligned} \quad (19)$$

where

$$\begin{aligned} \kappa_{\mathbf{k}} &= (h_1 - ih_2)/E_{\mathbf{k}}, \\ h_1 &= -t \left[\cos(k_x d) \cos(\sqrt{3}k_y d) + \cos(k_s d) \right], \\ h_2 &= -t \left[\sin(k_x d) \cos(\sqrt{3}k_y d) + \sin(k_s d) \right]; \end{aligned} \quad (20)$$

$f(E) = 1/(e^{\beta(E-\mu)} + 1)$ is the Fermi-Dirac distribution function, $\beta = 1/k_B T$, μ is a chemical potential. The energies are defined as

$$\begin{aligned} E_{\mathbf{k},l} &= E_{\mathbf{k},l}^{(1)} + E_{\mathbf{k},l}^{(2)}, \\ E_{\mathbf{k},l}^{(1)} &= (-1)^l \sqrt{h_1^2 + h_2^2} = \pm t \sqrt{3 + f(\mathbf{k})}, \\ E_{\mathbf{k},l}^{(2)} &= -t' f(\mathbf{k}) \end{aligned} \quad (21)$$

If we take $E_{\mathbf{k}}^{(2)} = E_{\mathbf{k}+\mathbf{q}}^{(2)} = 0$ the integral yields the same polarizability formula as that found in the nearest-neighbor model's polarizability [6, 7].

PLASMONS IN GRAPHENE

Plasmons are known as collective excitations of electrons, found from the equation

$$\epsilon(\mathbf{q}, \omega) = 0. \quad (22)$$

Complex solution of this equation $\omega(\mathbf{q})$ gives both the dispersion and the decay of plasmons. However, numerical solution of Eq. (22) for a complicated $\epsilon(\mathbf{q}, \omega)$, like that given by Eqs. (16) - (19) is challenging. That is why approximations schemes are used for analyzing the plasmon dispersion. One of them is based upon the loss function

$$Im\left(\frac{1}{\epsilon(\mathbf{q}, \omega)}\right) = \frac{-Im[\epsilon(\mathbf{q}, \omega)]}{\{Re[\epsilon(\mathbf{q}, \omega)]\}^2 + \{Im[\epsilon(\mathbf{q}, \omega)]\}^2}, \quad (23)$$

calculated as a function of real ω and \mathbf{q} . The peaks of the loss function are associated with the collective excitations of electrons (plasmons), thus giving real function $\omega(\mathbf{q})$. The other approximation is abridging Eq. (22) to the equation

$$Re[\epsilon(\mathbf{q}, \omega)] = 0, \quad (24)$$

which is solved for real function $\omega(\mathbf{q})$.

In the present paper the polarizability of graphene χ was evaluated numerically and the corresponding dielectric function is obtained from Eq. (16) for different values of the real frequency ω , the wave vector \mathbf{q} and chemical potential (Fermi energy) μ (κ was taken to be equal to 4.0). Comparison of our results with those of Ref. [6] shows that the next nearest-neighbor hopping strongly changes the shape of the plasmon curve for the low values of chemical potential μ . For high values of chemical potentials (higher than $3t'$, which is equal to the displacement of the Dirac nodes) the shape of the curves does not change much, but the plasmon curve becomes shorter. Thus the region of wave vectors, where plasmon can be observed, is reduced.

Plasmons near the saddle points appear on Fig. (8) and Fig. (9). The results were calculated only for the upper energy band where chemical potential is very close to the saddle points location. The figures correspond to the two values of $t' = 0.02, 0.2$ and like on other figures the direction of $q_x = 0.0$ is selected. The plasmons near the saddle points do not have the difference on the shape of the curve and look very similar to the other chemical potentials of the upper energy band.

The Fig. (10) compares the results of the two approximate methods of calculating the plasmon dispersion law, mentioned above. The loss function method has only one curve while the real part method has two curves. One curve of the real part method closely corresponds to that obtained by the loss function method, the other does not appear in the case of the loss function method calculations. The relevance of each of this curves can be analyzed by calculation of the imaginary part of the dielectric function in the vicinity of the curve. We see that for one curve given by Eq. (24) the imaginary part of ϵ is very low. And it is the curve which is given by the loss function method. In the vicinity of the other curve the

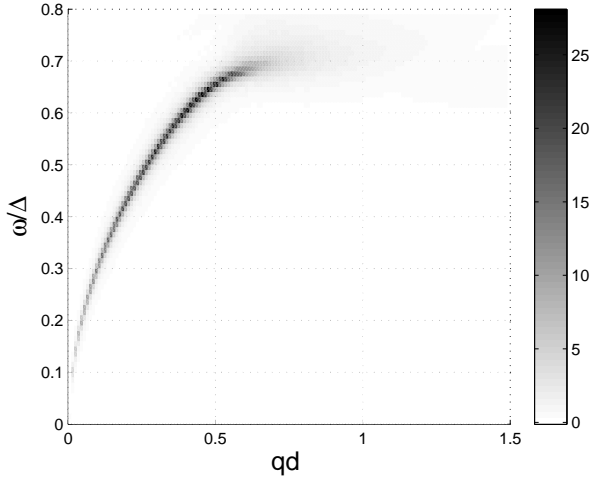


FIG. 3: Plasmon dispersion for $\mu = 1.44t, t' = 0.02t$ and different values of q_y component ($q_x = 0$)

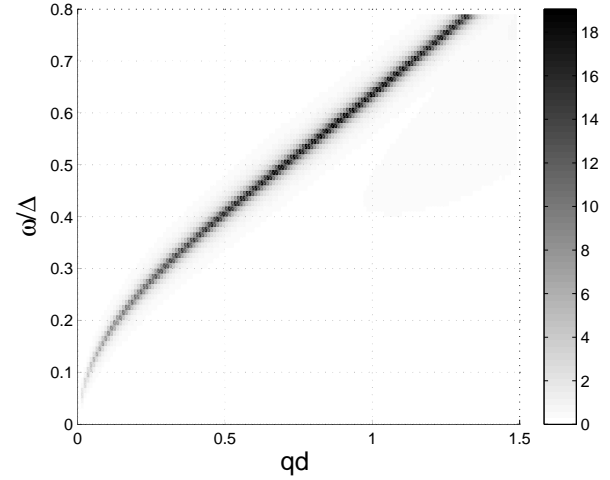


FIG. 5: Plasmon dispersion for $\mu = -2.82t, t' = 0.02t$ and different values of q_y component ($q_x = 0$)

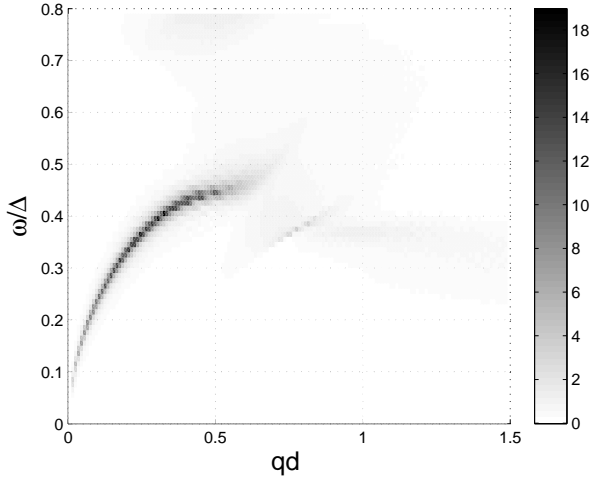


FIG. 4: Plasmon dispersion for $\mu = 0.9t, t' = 0.2t$ and different values of q_y component ($q_x = 0$)

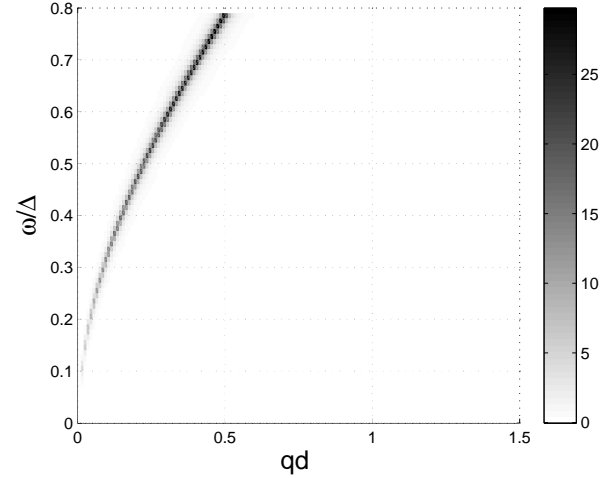


FIG. 6: Plasmon dispersion for $\mu = -3.36t, t' = 0.2t$ and different values of q_y component ($q_x = 0$)

imaginary part of ϵ is high, making it irrelevant. Thus the loss function is better choice for the calculation of plasmons.

-
- [1] A. H. Castro Neto, F. Guinea, N. M. R. Peres, K. S. Novoselov and A. K. Geim, *Rev. Mod. Phys.* **81**, 109 (2009).
 - [2] D.S.L. Abergel, V. Apalkov, J. Berashevich, K. Ziegler, T. Chakraborty, *Adv. Phys.* **59**, 261 (2010).
 - [3] B. Wunsch, T. Stauber, F. Sols and F. Guinea, *New J. Phys.* **8**, 318 (2006).
 - [4] E. H. Hwang and S. Das Sarma, *Phys. Rev B* **75**, 205418 (2007).
 - [5] M. Polini and R. Asgari and G. Borghi and Y. Barlas and

- T. Pereg-Barnea and A. H. MacDonald, *Phys. Rev. B* **77**, 081411(R) (2008).
- [6] A. Hill, S. A. Mikhailov, K. Ziegler, *EPL* **87**, 27005 (2009).
- [7] S. Yuan, R. Roldan, M. I. Katsnelson, *Phys. Rev. B* **84**, 035439 (2011).
- [8] E. Goursat, *Course D'Analyse Mathematique* [cited by Russian translation: *Kurs Matematicheskogo Analisa*, (Moscow 1933), Vol. I, Part 1, p 100.
- [9] P. R. Wallace, *Phys. Rev.* **71**, 622 (1947).

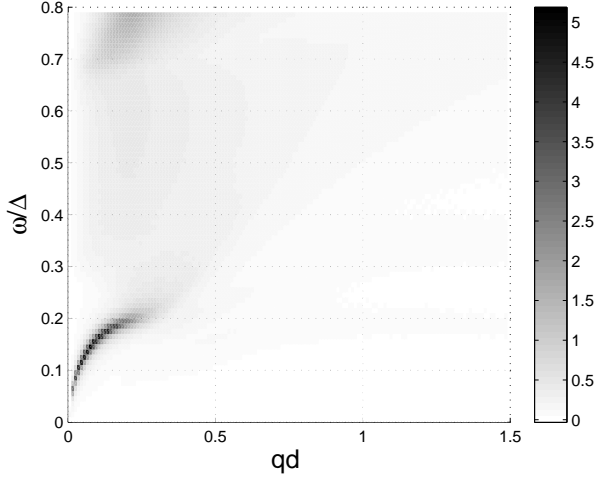


FIG. 7: Plasmon dispersion for $\mu = 0.4t, t' = 0.2t$ and different values of q_y component ($q_x = 0$)

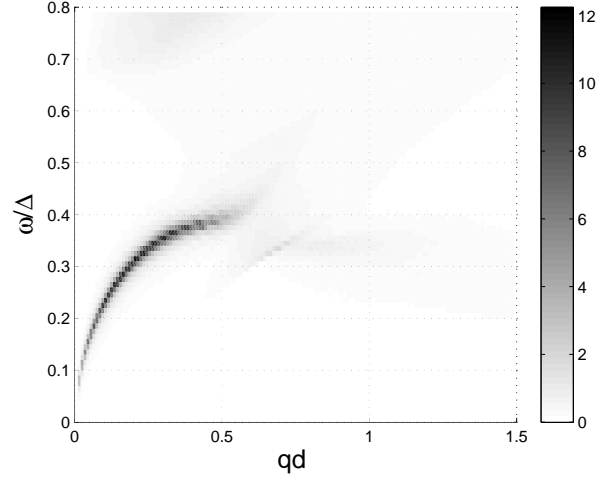


FIG. 9: Plasmon dispersion for the saddle point $\mu = 0.8t, t' = 0.2t$ and different values of q_y component ($q_x = 0$)

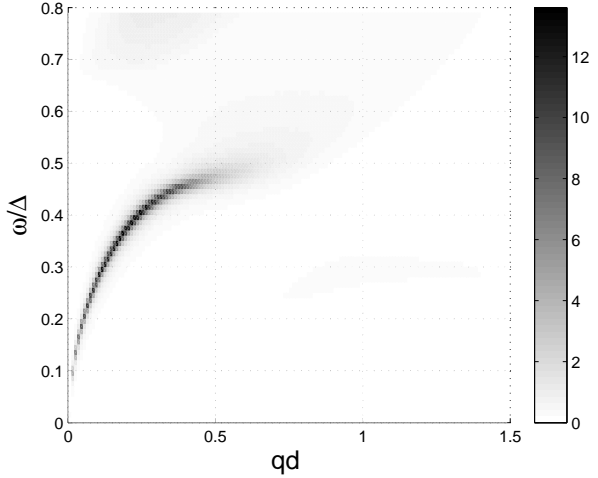
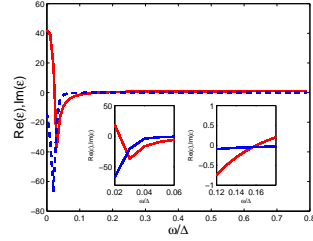
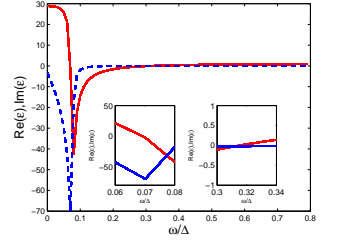


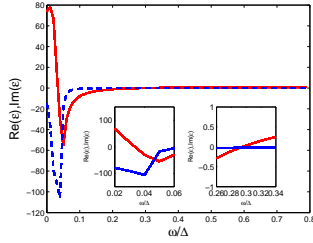
FIG. 8: Plasmon dispersion for the saddle point $\mu = 0.98t, t' = 0.02t$ and different values of q_y component ($q_x = 0$)



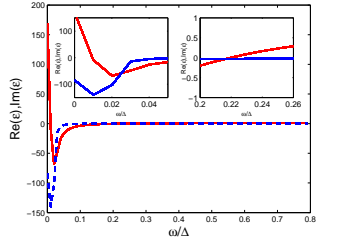
(a) $\mu = -0.94, t' = 0.02t, q_x = 0.1d^{-1}, d = 1.42\text{\AA}$



(b) $\mu = -1.12, t' = 0.2t, q_x = 0.1d^{-1}, d = 1.42\text{\AA}$



(c) $\mu = 0.48, t' = 0.02t, q_x = 0.1d^{-1}, d = 1.42\text{\AA}$



(d) $\mu = 0.3, t' = 0.2t, q_x = 0.1d^{-1}, d = 1.42\text{\AA}$

FIG. 10: Red curve represents the real part of dielectric function and blue curve represents imaginary part. Two small windows show areas where the real part of dielectric equals to zero. One window(right) shows that the imaginary part of dielectric like the real part equal to zero. The other window(left) shows that imaginary do not equals to zero but real part do.